Pflügers Arch. 364, 45–52 (1976)

Pflügers Archiv
European Journal of Physiology

Membrane Currents in the Rabbit Sinoatrial Node Cell as Studied by the Double Microelectrode Method *

AKINORI NOMA and HIROSHI IRISAWA

Department of Physiology, School of Medicine, Hiroshima University, Kasumicho, Hiroshima, Japan

Summary. When a strand of the rabbit sinoatrial node tissue was shortened by ligation, the spatial decay of electrotonic potential decreased and the input impedance increased. In a piece of the tissue 0.2–0.3 mm in diameter apparently uniform current spread was obtained. Action potentials recorded from three different sites in this small piece occurred simultaneously and were superimposable.

In voltage clamp experiments using the double microelectrode method, the membrane potential was usually held at −30 to −40 mV, where no net current flowed. When membrane potential was suddenly changed from the holding potential, the sign and the time course of the ionic current varied with membrane potential. Hyperpolarization gave an inward current which increased with time. Depolarization gave a transient inward current followed by sustained outward current, and repolarization gave an outward current tail which exponentially subsided with a time constant of 0.37 s.

The membrane time constant was 12.0 ms. When the specific membrane capacitance was assumed to be 1 $\mu F/cm^2$, the specific membrane resistance at the resting potential was 12 $k\Omega cm^2$. The peak of the transient inward current on depolarization was 1.3 $\times 10^{-5}$ A/cm^2.

Key words: Sinoatrial node cell – Voltage clamp – Inward current – Outward current tail – Current voltage relation.

INTRODUCTION

Most experiments on the sinoatrial node (S-A node) cell have been concerned with measurements of membrane potentials with microelectrodes (Brooks and Lu, 1972), and little effort has been made to measure the membrane current which is responsible for the pacemaker potential. Recently, the double sucrose gap method (Irisawa, 1972) and the single sucrose gap method (Noma and Irisawa, 1975; Seyama, 1976) were used in the voltage clamp experiment on the S-A node tissue. However, limitations of these methods became apparent when applied to the S-A node tissue because of a considerable amount of leakage current flow through the shunt resistance. Large leakage current leads to uncertainties in the magnitude of the membrane current in addition to inadequate control of membrane potential (New and Trautwein, 1972; McGuigan, 1974). This problem can be solved by employing the double microelectrode method (Deck et al., 1964), but the feasibility of this method still depends on the degree of success of the spatial clamp.

The cable properties of the S-A node tissue (Bonke, 1973; Seyama, 1976) may allow the membrane potential to be clamped by the double microelectrode method in a small S-A node specimen. Evaluation of spatial homogeneity in a small S-A node specimen and results of the voltage clamp experiment by the double microelectrode method will be described in this report.

METHODS

Rabbits, weighing 1.5–2.0 kg, were killed by a blow on the neck. After removing the right atrium, strips of the S-A node tissue 1 mm in length and 0.3 mm in width were made by dissecting the tissue in a direction perpendicular to the crista terminalis. The S-A node strips were placed in an organ bath having a capacity of 0.5 ml. The atrial muscles within the crista terminalis were removed, leaving the endocardial surface intact. The final thickness of the specimen was approximately 0.2–0.3 mm. After recording the membrane potential in this specimen, it was transected or ligated by a silk fiber into shorter strips in order to electrically isolate the pacemaking region from the remainder portion. Spontaneous activity resumed 10–30 min after each dissecting procedure. The

* This work was supported by the research grant from the Japanese Ministry of Education

smallest size of the specimen in which spontaneous activity recovered was 0.2–0.3 mm in length.

Routine microelectrodes filled with 3 M KCl were used both to record membrane potential and to apply current intracellularly. The membrane potential and current were displayed on an oscilloscope and were photographed. The principle of the feedback circuit for the voltage clamp was the same as that reported by Deck et al. (1964). The membrane potential was supplied to the summing point of the feedback amplifier (Analog Device 171K) having an output of ± 80 V and 10 mA. The current flowing through the current microelectrode was measured by means of a current voltage converter (Analog Device AD741). In one series of current clamp experiments, a bridge circuit (Araki and Otani, 1955) was used to measure the membrane potential through the current electrode.

A modified Tyrode aerated with 100% O_2 and kept at 35° C was continuously perfused through the organ bath at a rate of 2–3 ml/min. The composition of the Tyrode solution was NaCl 136.9, KCl 2.7, $CaCl_2$ 1.8, $MgCl_2$ 0.5, and NaH_2PO_4 1.3, in mM and its pH was adjusted to 7.4 by adding Na_2HPO_4.

The experimental values are given in mean ± S.D.

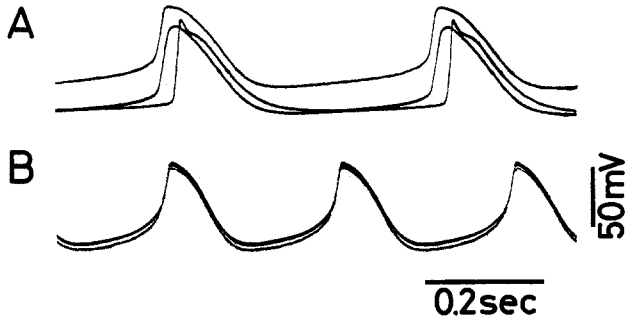

Fig. 1 A and B. Simultaneously recorded action potentials from 3 different sites within a specimen of 1 × 0.3 mm (A) and of 0.3 × 0.3 mm (B). In (A) 3 microelectrodes were arranged in a straight line at intervals of 340 and 500 μm. In (B) 3 adjacent electrodes were separated by 50–100 μm

RESULTS

Spontaneous Action Potentials in the Small S-A Node Specimen

Man-made S-A node strips 0.3 mm in width and longer than 0.5 mm showed spontaneous action potentials of normal shape and amplitude. The overshoot of the action potential was 10.3 ± 3.2 mV, the maximum diastolic potential 67.1 ± 3.6 mV, and the maximum rate of rise 5.5 ± 1.4 V/s in 12 experiments. Propagation of excitation was observed when the action potentials were simultaneously recorded at three different sites (Fig. 1 A). When the conduction velocity between these three recording sites was assumed to be constant, it was estimated to be 3.7 ± 1.5 cm/s in 17 experiments, which coincided well with the value reported by Sano and Yamagishi (1965).

When the specimen was made shorter, that is 0.3 mm in length, spontaneous activity recovered in approximately 70% of specimens within 30 min after transection or ligation. The action potentials obtained simultaneously from three different sites were superimposable (Fig. 1 B). The overshoot of the action potential was 7.0 ± 2.5 mV, the maximum diastolic potential 61.8 ± 3.5 mV, and the maximum rate of rise 3.6 ± 0.5 V/s in 4 experiments. These values were slightly smaller than those obtained in the longer specimens ($P < 0.01$).

If the conduction velocity in the small specimen is 3.7 cm/s, conduction time will be 2.7 ms for 0.1 mm of the tissue. However, the interval of the rising phase of the action potentials recorded at three sites located approximately 0.1 mm from each other was less than 0.5 ms. This fact indicates that in 0.3 mm specimen virtually no conduction took place. It is likely that during the slow diastolic depolarization phase the membrane potential of each cell became similar and the cells fired simultaneously.

Current Voltage Relationship in the Strands of Various Length

After having impaled three microelectrodes simultaneously, constant current pulses were applied through one electrode near the end of the strip and the electrotonic potentials at two different sites were recorded. When an anodal current was applied to a specimen 1.7 × 0.3 mm in size (Fig. 2 A), the shift of the maximum diastolic potential 0.1 mm away from the current feeding electrode was 7 times larger than that recorded at a distance of 0.3 mm, indicating that the electrotonic potential decayed rapidly along the length of the strand from the point form current source and the pacemaking site within the long specimen was nearly free from the effect of applied current. The frequency of the spontaneous activity slightly reduced from 202 to 185/min during the pulse (Fig. 2 A). When the current was applied to a specimen 0.7 × 0.3 mm in size (Fig. 2 B), the difference in magnitude of electrotonic potentials between two different sites was smaller than the difference obtained in the 1.7 × 0.3 mm specimen. Spontaneous activity ceased during application of anodal current pulse. After recording these tracings, a specimen 0.3 × 0.3 mm in size was prepared (Fig. 2 C). The current electrode was placed at the center of the specimen and the electrotonic potentials were recorded by two other electrodes placed 50–100 μm away from the central electrode. In this specimen, the two electrotonic potentials coincided with each other during application of cathodal (Fig. 2 C-1) and anodal (C-2) current.

Since the peak amplitude of the electrotonic potentials varied between different phases of the action potential, those measured during the diastolic phase

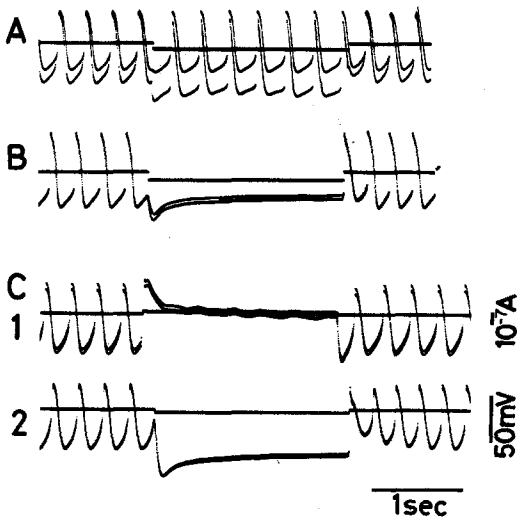

Fig. 2 A–C. Electrotonic potentials recorded from 2 different sites within the S-A node specimen. In (A) and (C) 2 traces of the membrane potential were not superimposed in the control. Size of the specimen was 1.7 × 0.3 mm in (A), 0.7 × 0.3 mm in (B) and 0.3 × 0.3 mm in (C). Recording electrodes were inserted 0.1 and 0.3 mm away from the current source in (A) and (B). In (C) 2 tonic potentials recorded at sites 50–100 μm away from the central current electrode coincided

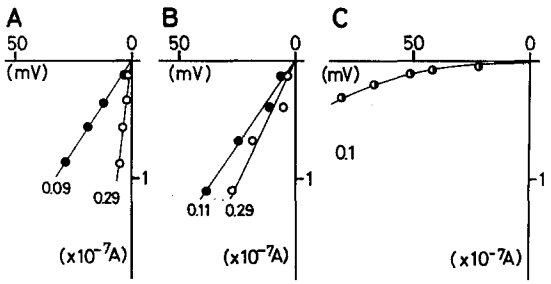

Fig. 3 A–C. Relation between the amplitude of the electrotonic potential and the applied current obtained from 3 specimens of different sizes, (A) 1.7 × 0.3 mm, (B) 0.7 × 0.3 mm, (C) 0.3 × 0.3 mm. Numerals in the graph indicate the distance between the recording electrode and the current electrode in mm. Abscissa: the peak amplitude of the electrotonic potentials. Half closed circles in C indicate that 2 electrotonic potentials coincided

(at around −50 mV) or in quiescent state (−35 to −40 mV) after ligation were plotted against the applied current. When the specimen was longer than 0.7 mm, linear relationships were obtained between these two variables (Fig. 3A, B), but in a specimen 0.3 mm in length nonlinear relationship was obtained (Fig. 3C). This fact suggests that cable complication tended to make the nonlineality less visible. The difference in amplitude of electrotonic potentials between two different sites became smaller as the specimen was made shorter (Fig. 3A and B). Finally, in all four 0.3 × 0.3 mm specimens two electrotonic potentials were of identical amplitude in a distance of 0.1 mm

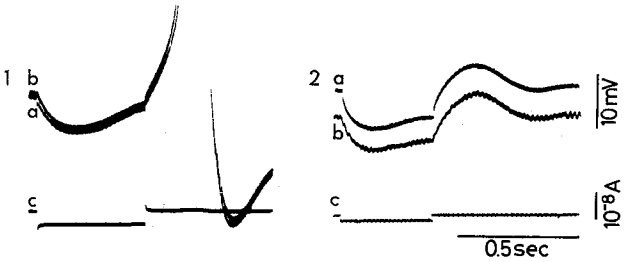

Fig. 4. Comparison of the membrane potential recorded from the current electrode using the bridge circuit (*a*) with that from the peripheral electrode 0.1 mm away from the current electrode (*b*). *c*: current record. In (1) only the lower part of the action potential is shown. In (2) the subthreshold oscillation followed the break of an anodal current pulse

(Fig. 3C). The input impedance estimated from the voltage shift at a point 0.1 mm away from the current electrode was 232 kΩ (ranging from 50–330 kΩ in 4 experiments) in a 1–2 mm specimen, while it was 1.4 MΩ in a 0.3 mm specimen (ranging from 500 kΩ to 4 MΩ in 6 experiments). Transection of the specimen from 1–2 mm to 0.3 mm increased the input impedance on the average by a factor of 6.1.

Equivalent Circuit for the Smallest S-A Node Specimen

The foregoing results suggest that the smallest S-A node specimen behaves like a single cell. However, it is still possible that the electrotonic potential decays rapidly in the vicinity of the current electrode because of a three dimensional spread of the applied current. The trace of the membrane potential recorded through the current electrode using the bridge circuit method was almost superimposable with that recorded at a peripheral site of the specimen (Fig. 4). In 9 experiments, the magnitude of the electrotonic potentials (ranged from 3–8 mV) at the peripheral electrode was 94 ± 4% of that recorded at the current electrode. Therefore, the spatial homogeneity of the membrane potential within a 0.3 mm specimen was confirmed near the resting membrane potential. Furthermore, there was no apparent sharp voltage step in the potential record (inset trace in Fig. 5) at the onset of the current pulse application, indicating that the series resistance was negligibly small in the S-A node specimen. Therefore, the time constant of this specimen is almost equal to the membrane time constant. If a constant current is applied to a specimen in which spatial homogeneity is achieved, the amplitude of the electrotonic potential (V) at time t from the onset of the pulse is given by the equation (modified from Hodgkin and Rushton, 1946)

$$V = V_\infty (1 - e^{-t/\tau})$$

where V_∞ is the potential change at infinite time and

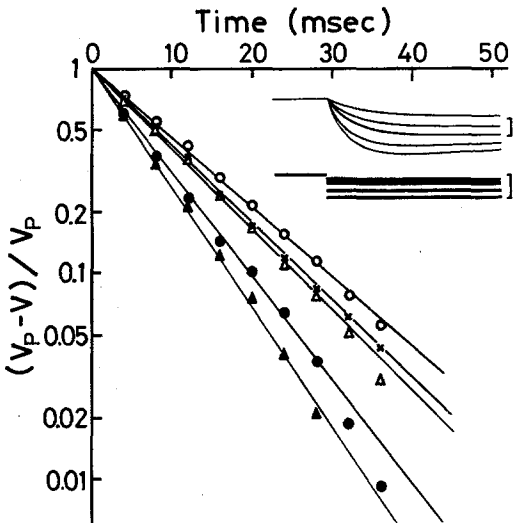

Fig. 5. Exponential potential change during anodal current pulse. Different symbols indicate the electrotonic potentials of different amplitudes. The inset tracings are the potential record (upper trace) and the current record (lower trace). Upper vertical bar is 10 mV and lower bar 5×10^{-8} A. Duration of the pulses was 80 ms

Table 1. Electrical constants of the S-A node cell membrane. The membrane time constant (τ) was measured in the way shown in Figure 5. Input impedance (r) were computed from the amplitude of the tonic potential (V) and the applied current. Total capacitance of the specimen was obtained from τ/r. M.P. is the resting potential

	τ(ms)	r(MΩ)	c(nF)	V(mV)	M.P.(mV)
1	12.4	2.33	5.3	10.5	35.5
2	12.6	3.33	3.8	10.0	40.0
3	11.0	1.74	6.3	16.5	42.0
4	10.6	1.37	7.6	14.5	41.4
5	13.0	1.80	7.2	9.0	27.8
6	12.2	2.32	5.3	6.5	38.0
mean	12.0	2.15	5.9	–	–

τ is the membrane time constant. From this equation

$$\log [(V-V_\infty)/V_\infty] = k \cdot t/\tau$$

where k is constant. In quiescent specimens the time constant of the development of the electrotonic potential was studied as in Figure 5, where $\log [(V-V_p)/V_p]$ was plotted against t. V_p is the peak amplitude of the electrotonic potential and was used as an approximate value of V_∞. The potential change within 20 ms after the onset of the current was expressed by a straight line. The slope of the line was steeper as V_p became larger. This fact indicates that the time constant decreased as the magnitude of the electrotonic potential increased. Because the membrane resistance decreased when the membrane was hyperpolarized (Fig. 8), τ might have decreased. Time constant, input impedance and membrane capacitance in 6 experiments are given in Table 1. Assuming that all the capacitance of the specimen is on the surface membrane and that the specific membrane capacitance is 1 μF/cm² (Weidmann, 1970; Kamiyama and Matsuda, 1966; Sakamoto and Goto, 1970), then the total membrane surface of a 0.3×0.3 mm specimen will be 5.9×10^{-3} cm² and the specific membrane resistance 12 kΩcm². The individual myocardial cells in the S-A node tissue are spindle shaped (Trautwein and Uchizono, 1963; Virágh and Porte, 1973), approximately 10 μm in largest diameter and 50 μm from end to end. Assuming the surface area of a single cell to be 1730×10^{-8} cm², about 350 cells will be included in an specimen of 0.3×0.3 mm.

Voltage Clamp Experiments

Spatial homogeneity of the clamp potential throughout the small specimen was tested by measuring the membrane potential at a peripheral site by a third microelectrode which was not included in the control circuit (Fig. 6). At the beginning of the record, the membrane potential was clamped at a potential equivalent to the resting membrane potential (reference potential; Noma and Irisawa, 1975). Approximately 2 s after clamping to −40 mV, a depolarizing clamp step of 11 mV was applied for 2.1 s. The potential from the voltage controlling electrode coincided well with that from the third monitoring electrode. When the membrane was depolarized by 36.5 mV in the same preparation, the two recorded step potentials differed only by 0.8 mV. These results suggest that a virtually satisfactory voltage clamp was achieved in the small S-A node specimen. When the membrane was released from the clamping circuit, it depolarized very slowly and an action potential was initiated. A similar sequence of procedure was repeated in the following voltage clamp experiments, omitting the third electrode.

Figure 7 shows the membrane potential and membrane current during different clamp steps from a holding potential of −35 mV in normal Tyrode. When step changes to −53 and −25 mV were made, tracings of the capacitative current tail for anodal and cathodal changes were almost symmetrical. The charging process was virtually completed in 5–10 ms in all traces. On depolarization, the capacitative surge was followed by a transient inward current. The threshold for the inward current was 3–5 mV positive to the holding potential. With increasing depolarization in the range from −25 to −7 mV, the time course of activation of the inward current became faster. Finally, the peak of the inward current appeared 5 ms after the onset of depolarization to 12 mV. Therefore, the peak of the inward current at potentials more positive

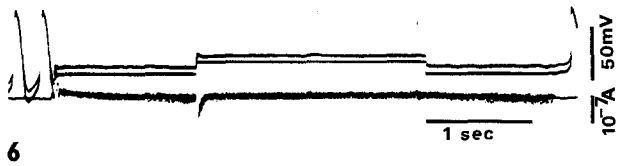

Fig. 6. Spatial uniformity of the voltage control. Top trace was recorded from the third microelectrode which was not included in the feedback circuit, middle trace clamp potential, and bottom trace current record. Note the outward current tail on clamping to the holding potential, and the initiation of the action potential on switching off the feed back circuit. Size of the specimen was slightly larger than 0.3×0.3 mm

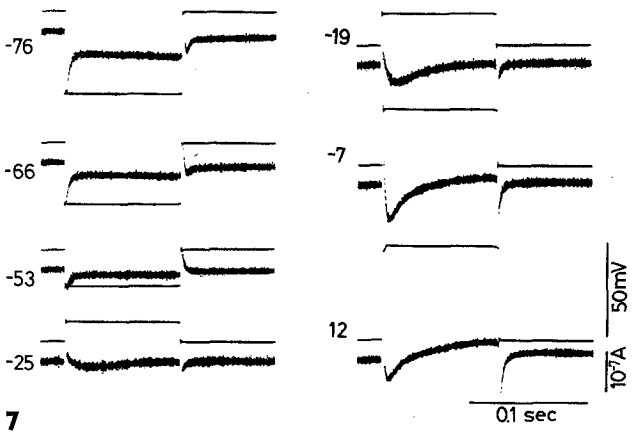

Fig. 7. Membrane currents in Tyrode solution. Upper trace indicates the clamp potential, lower trace gives the current trace in each record. Holding potential was -35 mV, at which no net current was observed in a steady state. Displacement of the membrane potential was indicated in mV at the left side of each record. For initial 5 ms of the clamp pulse at 12 mV, membrane potential was not clamped due to the limitation of the current supply. Size of the specimen was 0.3×0.2 mm

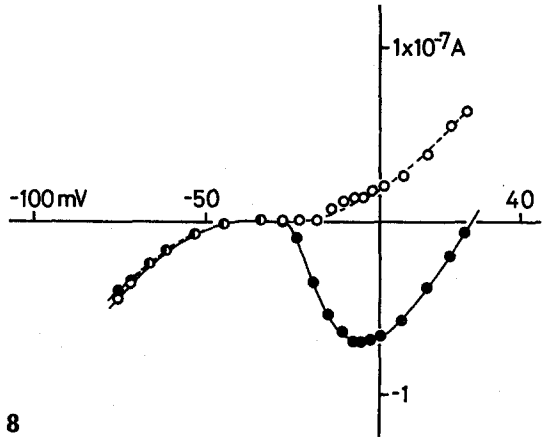

Fig. 8. Current voltage relation at 10 ms after the onset of the voltage step (filled circles) and at 100 ms (open circles). Transient inward current was plotted at its peak. Measurements were made from the records reproduced in Figure 7

than 12 mV might be overlapped by the tail of the capacitative surge. A slowly increasing outward current followed the transient inward current and on repolarization the outward current tail declined very slowly.

On hyperpolarization an inward current flowed and its magnitude slowly increased with time during the clamp step. On clamping back to the holding potential, an inward current tail was observed (Fig. 7). In different examples an inverted action potential wave form was frequently observed in the current trace, which is characteristic of escape from clamp control.

The peak amplitude of the transient inward current during depolarization and the amplitude of the inward current 10 ms after hyperpolarization were plotted against the membrane potential in Figure 8 (closed circles). The maximum value of the transient inward current was reached at around -5 mV and was $7.7 \pm 1.2 \times 10^{-8}$ A in 6 experiments. The positive slope of the current voltage curve intersects the abscissa at 29.2 ± 4.9 mV in 6 experiments. The reversal potential of the transient inward current, however, may be more positive because the inward current was overlapped by an appreciable capacitative surge, leakage current and other time dependent current.

Open circles in Figure 8 represent the current 0.1 s after the onset of the clamp pulses, when the inward current was largely inactivated. Delayed rectification became apparent when the membrane was clamped to potentials positive to -20 mV. When the membrane was hyperpolarized beyond -50 mV, there was a considerable increase of membrane conductance.

Figure 9 shows slow current changes during and after the clamp pulses. During the clamp pulses, a steady state of the membrane current was not observed, but a quasi-stable state was reached 0.5 s after the onset of the depolarizing pulses. The greater the magnitude of hyperpolarization, the larger and faster was the change in magnitude of the inward current. The outward current tail on repolarization decayed with a time constant of 0.37 s at -40 mV (average of 3 experiments).

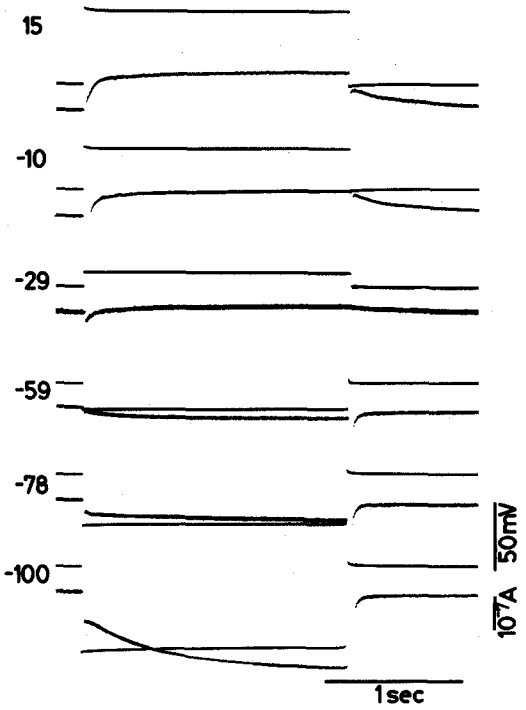

Fig. 9. Membrane currents during relatively long voltage clamp pulses. Upper traces are the membrane potentials and lower traces are the membrane current. Holding potential was −40 mV. Displacement of the membrane potential was indicated in mV at the left side of each record

DISCUSSION

The S-A node tissue has cable properties in spite of the small number of nexus connections between the adjacent cells (Virágh and Porte, 1973) and the applied current spreads with a space constant of 0.5–0.8 mm (Bonke, 1972; Seyama, 1976). In accordance with this property, the input impedance of the membrane increased and the slope of spatial decay of the electrotonic potential decreased as the length of the tissue strand was reduced. Increase of the input impedance is expected from the following equation (Weidmann, 1952),

$$V_o/I_o = r_i \lambda \coth (L/\lambda)$$

where V_o is the electrotonic potential at the current electrode, I_o the applied current, r_i the resistance of the core per unit length, λ the space constant, and L the length of the specimen. If λ is assumed to be 0.8 mm, V_o/I_o in a 0.3×0.3 mm specimen is 2.5 times larger than that in a 1.0×0.3 mm specimen. In this experiment, however, the input impedance increased by a factor of 6.1 when a 1 mm specimen was transected into a 0.3 mm specimen.

On the other hand, decrease in the slope of spatial decay of the electrotonic potential (V) at x mm from the current electrode is expected from the following equation (Weidmann, 1952),

$$V = V_o \frac{\cosh [(L-x)/\lambda]}{\cosh (L/\lambda)}.$$

In a 0.3 mm specimen, the magnitude of the electrotonic potential at the peripheral site of the specimen is 96.5% of the value at the central current electrode. In this study, it was 94 ± 4% of the maximum value and agreed well with the expected value.

During the transient inward current phase, however, the maximum chord conductance in 5 experiments was approximately 10 times larger than the resting membrane conductance. Therefore, λ might have been reduced to 35% of that in the resting condition, and nonuniform distribution of potential might have existed during the peak inward current. However, the present experiments suggest that this is unlikely. The depolarization step of 36.5 mV caused a difference of only 0.8 mV between the two monitoring potentials in spite of the increased membrane conductance due to the delayed rectification. Moreover, at the beginning of the depolarizing step, the wave form characteristic of escape from clamp control was not recorded in the potential record by the third elctrode. The current clamp experiments shown in Figure 2 also indicate a uniform potential distribution even under conditions of high membrane conductance. These results imply either that the surviving region was smaller than the apparent size of the specimen or that the space constant was longer than 0.8 mm in this specimen.

The transient inward current of the S-A node cell was slow compared to the fast inward current of other myocardial fibers, but its time course was similar to that of the slow inward current (Rougier et al., 1969; Beeler and Reuter, 1970; New and Trautwein, 1972). The transient inward current of the S-A node cell was not preceded by a fast inward current. The fact that the rising phase of the S-A node action potential continued for approximately 10–20 ms is in good accord with the result that the inward current phase continued for approximately 30 ms at 0 mV. It is unlikely that the slow time course of the transient inward current in the S-A node cell might have resulted from inadequacies in the spatial and temporal control of the membrane potential (Johnson and Lieberman, 1971).

Since the total membrane capacitance of the specimen was 6×10^{-9} F and the maximum rate of rise of the action potential was about 5 V/s, the peak inward current would be 3×10^{-8} A. The measured value was approximately 8×10^{-8} A in this experiment and the two values were of the same order of magnitude. When the total membrane surface of a 0.3×0.3 mm

specimen is assumed to be 6×10^{-3} cm^2, the current density will be 1.3×10^{-5} A/cm^2. This value is about 1/100 of that in the squid giant axon (Hodgkin and Huxley, 1952). From these estimates, it seems appropriate to conclude that the inward current of the S-A node cell is small and slow.

The major ion responsible for the slow inward current in the ventricle is Ca (Beeler and Reuter, 1970; Ochi, 1970; New and Trautwein, 1972). However, participation of Na ion in the maximum rate of rise of the S-A node cell was described previously (Noma and Irisawa, 1974). An increase of the extracellular concentration of Ca ion caused a parallel shift of the inactivation curve to positive potential without changing the highest value of the maximum rate of rise (Noma and Irisawa, 1976) as in Purkinje fibers (Weidmann, 1955). In preliminary experiments it was observed that the transient inward current in 30% $[Na]_o$ was approximately 3 times smaller than that in control Tyrode. Therefore, the transient inward current in the S-A node cell might be carried by Na ion.

The present voltage clamp experiments of the S-A node cell confirmed the previous results obtained by using the sucrose gap method (Irisawa, 1972; Noma and Irisawa, 1975; Seyama, 1976) in the following respects. 1. No repetitive spontaneous current change was observed during the voltage clamp. Thus, the membrane current is mostly dependent upon voltage and time. 2. A progressively increasing inward current was observed during the hyperpolarizing clamp step. On repolarization after the depolarization, a residual outward current tail was observed. The outward current tail in the S-A node tissue is in good accord with that in the mammalian Purkinje fiber (Deck and Trautwein, 1964; Noble and Tsien, 1968). In the S-A node cells the outward current appears to be carried by K ion as in Purkinje fiber (Seyama, 1976). 3. The current voltage relation shows a low membrane conductance in the potential range between -60 and -20 mV.

It appears difficult to explain the inward current changes during and after the hyperpolarizing pulses (Fig. 7). These conductance changes may not be solely attributable to the deactivation and activation of the potassium current as in the Purkinje fiber (Noble and Tsien, 1968), since the amplitude of the current change gradually increased as the test hyperpolarizing pulses were increased (Fig. 9), and the time course of the inward current tail was faster than the outward current tail. More than one conductance system or depletion of the extracellular potassium might have been involved in the current changes during and after the hyperpolarizing pulses. Alternatively, it might be possible that the inward current tail was an artifact due to the excitatory inward current, because its inactivation should be removed during hyperpolarization. However, the inward current tail in Figure 7 was obviously smaller in magnitude and shorter in duration than the inverted action potential wave form.

It has been suggested that the resting potential of the S-A node cell is lower than the maximum diastolic potential (Trautwein and Dudel, 1958) and is -38.4 ± 3.1 mV (Noma and Irisawa, 1975). In the absence of feed-back, the outward current tail after depolarization would have hyperpolarized the membrane beyond the resting potential and produced a positive after potential. The deactivation of the outward current has been suggested as the cause of the pacemaker potential (Weidmann, 1956; Dudel and Trautwein, 1958; Vassalle, 1966). During the hyperpolarization the outward current system may be switched off and the excitatory sodium current may be progressively activated (McAllister, Noble and Tsien, 1975). However, these systems are insufficient to explain how the S-A node cells initiate the spontaneous activity after a quiescent period (as shown in Fig. 6 in this experiment and in Fig. 8 and 9 in Noma and Irisawa, 1975). Because of the small membrane conductance at the resting potential, any small change in current will evoke oscillation of the membrane potential. The rectifier property shown in the Purkinje fiber (Noble and Tsien, 1968) might also be involved in slow depolarization after a quiescent period.

Acknowledgment. We are indebted to Dr. I. Seyama for valuable comments.

REFERENCES

Araki, T., Otani, T.: Response of single motoneurones to direct stimulation in toad's spinal cord. J. Neurophysiol. **18**, 472–485 (1955)

Beeler, G. W., Jr., Reuter, H.: Membrane calcium current in ventricular myocardial fibres. J. Physiol. (Lond.) **207**, 191–209 (1970)

Bonke, F. I. M.: Electrotonic spread in the sinoatrial node of the rabbit heart. Pflügers Arch. **339**, 17–23 (1973)

Brooks, C. McC, Lu, H. H.: The sinoatrial pacemaker of the heart. Springfield, Ill.: Ch. C. Thomas 1972

Deck, K. A., Kern, R., Trautwein, W.: Voltage clamp technique in mammalian cardiac fibres. Pflügers Arch. ges. Physiol. **280**, 50–62 (1964)

Deck, K. A., Trautwein, W.: Ionic currents in cardiac excitation. Pflügers Arch. ges. Physiol. **280**, 63–80 (1964)

Dudel, J., Trautwein, W.: Der Mechanismus der automatischen rhythmischen Impulsbildung der Herzmuskelfaser. Pflügers Arch. ges. Physiol. **267**, 553–565 (1958)

Hodgkin, A. L., Huxley, A. F.: A quantitative description of membrane current and its application to conduction and excitation in nerve. J. Physiol. (Lond.) **117**, 500–544 (1952)

Hodgkin, A. L., Rushton, W. A. H.: The electrical constants of a crustacean nerve fibre. Proc. roy. Soc. B **133**, 444–479 (1946)

Irisawa, H.: Electrical activity of rabbit sino-atrial node as studied by a double sucrose gap method. In: Proceedings of the satellite symposium of the XXVth international congress of physiological

sciences: The electrical field of the heart. (P. Rijlant, ed.). Bruxelles: Presses Academiques Europeenes 1972
Johnson, E. A., Lieberman, M.: Heart: Excitation and contraction. Ann. Rev. Physiol. **33**, 479–532 (1971)
Kamiyama, A., Matsuda, K.: Electrophysiological properties of the canine ventricular fiber. Jap. J. Physiol. **16**, 407–420 (1966)
McAllister, R. E., Noble, D., Tsien, R. W.: Reconstruction of the electrical activity of cardiac Purkinje fibres. J. Physiol. (Lond.) **251**, 1–59 (1975)
McGuigan, J. A. S.: Some limitations of the double sucrose gap, and its use in a study of the slow outward current in mammalian ventricular muscle. J. Physiol. (Lond.) **240**, 775–806 (1974)
New, W., Trautwein, W.: Inward membrane currents in mammalian myocardium. Pflügers Arch. **334**, 1–23 (1972)
Noble, D., Tsien, R. W.: The kinetics and rectifier properties of the slow potassium current in cardiac Purkinje fibres. J. Physiol. (Lond.) **195**, 185–214 (1968)
Noma, A., Irisawa, H.: The effect of sodium ion on the initial phase of the sinoatrial pacemaker action potentials in rabbits. Jap. J. Physiol. **24**, 617–632 (1974)
Noma, A., Irisawa, H.: Effects of Na^+ and K^+ on the resting membrane potential of the rabbit sinoatrial node cell. Jap. J. Physiol. **25**, 287–302 (1975)
Noma, A., Irisawa, H.: Effects of calcium ion on the rising phase of the action potential in rabbit sinoatrial node cells. Jap. J. Physiol. **26**, 93–99 (1976)
Ochi, R.: The slow inward current and the action of manganese ions in guinea-pig's myocardium. Pflügers Arch. **316**, 81–94 (1970)
Rougier, O., Vassort, G., Garnier, D., Gargouil, Y. M., Coraboeuf, E.: Existence and role of a slow inward current during the frog atrial action potential. Pflügers Arch. **308**, 91–110 (1969)
Sakamoto, Y., Goto, M.: A study of the membrane constants in the dog myocardium. Jap. J. Physiol. **20**, 30–41 (1970)
Sano, T., Yamagishi, S.: Spread of excitation from the sinus node. Circulat. Res. **16**, 423–430 (1965)
Seyama, I.: Characteristics of the rectifying properties of the sino-atrial node cell of the rabbit. J. Physiol. (Lond.) **255**, 379–397 (1976)
Trautwein, W., Dudel, J.: Hemmende und „erregende" Wirkungen des Acetylcholin am Warmblüterherzen. Zur Frage der spontanen Erregungsbildung. Pflügers Arch. ges. Physiol. **266**, 653–664 (1958)
Trautwein, W., Uchizono, K.: Electron microscopic and electrophysiologic study of the pacemaker in the sino-atrial node of the rabbit heart. Z. Zellforsch. **61**, 96–109 (1963)
Vassalle, M.: Analysis of cardiac pacemaker potential using a "Voltage clamp" technique. Amer. J. Physiol. **210**, 1335–1341 (1966)
Virágh, Sz., Porte, A.: The fine structure of the conducting system of the monkey heart (*Macaca mulatta*) I. The sino-atrial node and the internodal connections. Z. Zellforsch. **145**, 191–211 (1973)
Weidmann, S.: The electrical constants of Purkinje fibres. J. Physiol. (Lond.) **118**, 348–360 (1952)
Weidmann, S.: Effects of calcium ions and local anaesthetics on electrical properties of Purkinje fibre. J. Physiol. (Lond.) **129**, 568–582 (1955)
Weidmann, S.: Elektrophysiologie der Herzmuskelfaser. Bern-Stuttgart: H. Huber 1956
Weidmann, S.: Electrical constants of trabecular muscle from mammalian heart. J. Physiol. (Lond.) **210**, 1041–1054 (1970)

Received December 6, 1975